ELSEVIER

Composites: Part A 32 (2001) 1263–1270

composites
Part A: applied science and manufacturing

www.elsevier.com/locate/compositesa

Effect of impact damage on the compressive response of composite laminates

V.J. Hawyes[a], P.T. Curtis[a], C. Soutis[b,*]

[a]Mechanical Sciences Sector, DERA Farnborough, Hampshire GU14 0LX, UK
[b]Department of Aeronautics, Imperial College of Science, Technology and Medicine, Prince Consort Road, London SW7 2BY, UK

Received 21 March 2000; revised 10 October 2000; accepted 17 October 2000

Abstract

At present, the compressive strength of composite laminates containing an open-hole can be predicted theoretically by using fracture mechanics based models such as the linear softening cohesive zone model. In this approach, the inelastic deformation associated with fibre microbuckling that develops near the hole edge is replaced with an equivalent crack loaded on its faces by a bridging traction which is linearly reduced with the crack closing displacement. By making use of this model, and by establishing an equivalent hole diameter from X-radiographs and/or ultrasonic C-scan images, the residual compressive strength after impact can be predicted. This paper outlines how the 'equivalent hole' is determined and gives tabulated results of experimental and theoretical data. It is also shown that these data are in good agreement with each other for plain compression, open-hole compression and compression after impact strengths.

Keywords: A. Polymer-matrix composites (PMCs); Residual strength; C. Micro-mechanics

1. Introduction

One of the major factors limiting the design of structures made from current carbon fibre-epoxy systems is the susceptibility of the material to impact damage in the form of matrix cracking, multiple delaminations and fibre breakage. Low energy impacts may arise on aircraft structures due to dropped tools, runaway debris and hail-stones. The localised damage is termed barely visible impact damage (BVID) and is potentially a source of mechanical weakness, particularly under compression loading. Considerable research has, therefore, been devoted to analysing the impact properties and post-impact compression behaviour with a view to improving impact energy tolerance.

A theoretical model such as the cohesive zone model [1] can be used to predict the open-hole compressive strength of a composite laminate failing by 0° fibre microbuckling (Fig. 1). This model can also be used to predict the residual compressive strength of a material after impact damage [2]. The area of damage, determined from X-radiographs and/or C-scans, is used as an equivalent open hole.

In this work two materials, Toray T800 fibre in Hexcel 924 resin and Hexcel IMS/M21, and four stacking sequences $[\pm 45,0,90]_{2s}$, $[(\pm 45°,0°_2)_2]_s$, $[(45,0,-45,90)_{4s}]$ and $[(0,\pm 45,0,90,0,\pm 45,0,90,0,\pm 45,0)_s]$, have been examined. All IMS/M21 data (stacking sequence 8 in Table 1) and some T800/924 data have been obtained as part of the testing programme for this project. Other T800/924 data have been drawn from literature. Results that were obtained using the theoretical model have been compared to experimental data and are recorded in a tabular format. The percentage error between the two is also given.

2. Materials and mechanical tests

Both T800/924 and IMS/M21 fibre–resin systems are manufactured as prepreg material by Hexcel. T800/924 is a commonly used aerospace fibre–resin system consisting of intermediate modulus carbon fibres and a toughened epoxy matrix. IMS/M21 is a modern interleaved system with relatively new toughened epoxy resin and intermediate modulus carbon fibres. Each panel was laid up and auto-clave-cured according to manufacturer's instructions at DERA Farnborough. After manufacture, all panels were C-scanned to ensure panel integrity.

* Corresponding author. Tel.: +44-20-7594-5070; fax: +44-20-7584-8120.
E-mail address: c.soutis@ic.ac.uk (C. Soutis).

1359-835X/01/$ - see front matter
PII: S1359-835X(01)00072-0

Nomenclature

β	kink band inclination (°)
ϕ	fibre waviness (°)
d	diameter of (drilled) hole (mm)
a	diameter of equivalent hole (mm)
w	width of test piece (mm)
K_c	in-plane fracture toughness (MPa$\sqrt{m}$)
σ^{∞}	applied stress (MPa)
σ_{un}^{th}	theoretical unnotched (plain) compressive strength (MPa)
σ_{n}^{th}	theoretical notched (open-hole) compressive strength (MPa)
σ_{CAI}^{th}	theoretical compression after impact strength (MPa)
σ_{un}^{exp}	experimental unnotched (plain) compressive strength (MPa)
σ_{n}^{exp}	experimental notched (open-hole) compressive strength (MPa)
σ_{CAI}^{exp}	experimental compression after impact strength (MPa)

For ease of recording results, the different systems examined will be referred to as lay-ups 1–8 as recorded in Table 1. Stacking sequences 1–7 refer to T800/924 systems, whilst stacking sequence 8 corresponds to IMS/M21 system.

Mechanical tests have been carried out over several programmes. Some data have been drawn from published literature, others have been tested during the course of this programme. All tests followed standard procedures for mechanical testing. The unidirectional compressive strength was determined by a Celanese-type test rig. This is a test designed to eliminate macro-instability by means of a carefully designed jig and test-piece. The choice of jig can affect the accuracy of the results obtained. Open-hole compression, impact and compression after impact tests were carried out on coupons from each material and stacking sequence according to the CRAG test methods [3].

All test-piece coupons were cut to size with a diamond-slitting saw and, where appropriate, end tabs were bonded to each coupon with Redux 403 adhesive.

A hole of known diameter was drilled in the centre of each open-hole compression test-piece using a tungsten carbide tipped tool. Impact damage was introduced by using a hemispherical indentor on a Rosand Instrumented dropweight machine. All panels were ultrasonically C-scanned after impact to assess the extent of damage. Some were also examined by penetrant enhanced X-ray radiographs.

Residual compressive strength tests for both impact-damaged and open-hole test-pieces were performed using an appropriate anti-buckling guide to prevent macro-instability [3,4].

Table 1
Material and stacking sequence for each lay-up

T800/924	$[(\pm 45,0,90)_2]_s$	Lay-up 1
	$[(0, \pm 45,0,90,0, \pm 45,0,90,0, \pm 45,0)]_s$	lay-up 2
	$[(45,0, -45,90)_4]_s$	lay-up 3
	$[(\pm 45,0_2)_2]_s$	lay-up 4
	$[((\pm 45)_2,0_4)]_s$	lay-up 5
	$[(45,0, -45,0)_2]_s$	lay-up 6
	$[(0_2, \pm 45)_2]_s$	lay-up 7
IMS/M21	$[(\pm 45,0,90)_2]_s$	Lay-up 8

3. Experimental results

3.1. Unidirectional compression

The specimens were end-tabbed and of gauge section 10 mm × 10 mm; this gauge length is sufficiently short for an antibuckling guide not to be required. Two strain gauges were attached to the test-piece back-to-back to monitor any potential bending. Fig. 2 gives typical Celanese-type stress versus strain curves for T800/924C 16-ply unidirectional specimens with and reduced amount of Euler bending. Similar observations were made for the IMS/M21 system. Unnotched or undamaged test-pieces are difficult to test in compression because they are very susceptible to Euler buckling, misalignments and high stress concentration factors near the end tabs.

Recent results acquired by Hawyes et al. [5] gave low values of compressive strength when compared to results recorded by Soutis et al. [6,7]. The main reason for this discrepancy is the amount of bending observed in the test-piece when tested using the DERA modified jig (Fig. 2a). Less amount of bending was observed in the test-pieces of Soutis et al. [6,7] where a slightly different design of jig was employed (Fig. 2b). Table 2 gives the average results for unidirectional strength for the two materials. At least five tests were performed for each composite system and the coefficient of variation was less than 10%.

3.2. Plain and open-hole compression

The mean plain (i.e. unnotched) compressive strengths of the multidirectional (MD) laminates for the different stacking sequences examined in this study are recorded in Table 3 together with strength data obtained in previous work [8–10]. The result for lay-up 8 is low due to bending of the test-piece that led to premature grip failure.

Table 2
Mean unidirectional compressive strengths

Lay-up	UD compressive strength (MPa)
T800/924 UD	1082[a], 1350[b], 1430[c]
IMS/M21 UD	1021[a]

[a] Hawyes et al. [5].
[b] Soutis et al. [6].
[c] Soutis [7].

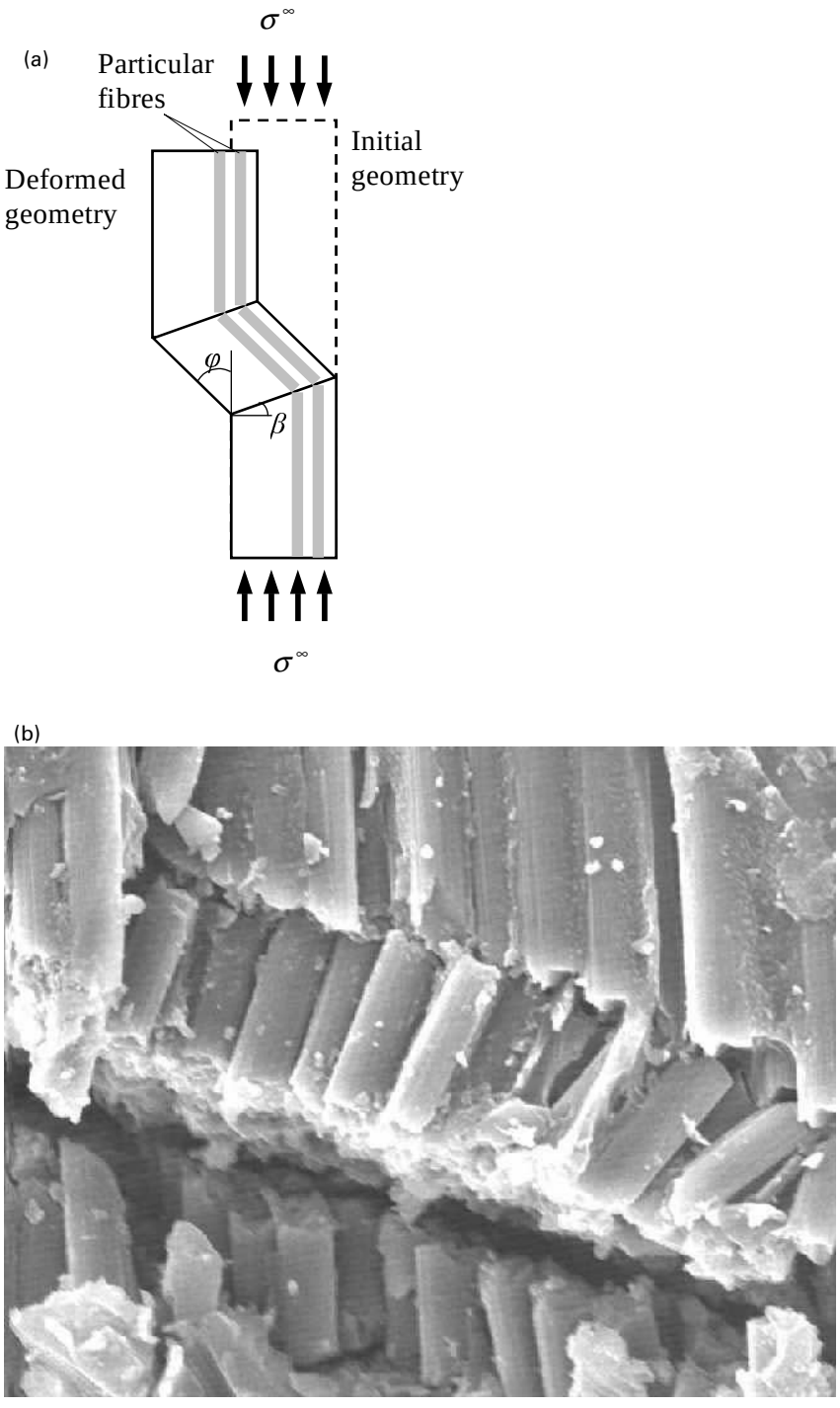

Fig. 1. (a) A schematic of fibre microbuckling. (b) A micrograph of fibre microbuckling.

The presence of a notch or hole in a component whilst in service is almost inevitable. It may arise as a result of a joint, an access opening or a cut-out used to reduce weight in the structure. Its presence will reduce the compressive strength as it gives rise to a stress concentration factor [1]. The ratio between hole diameter, d and width, w does affect the strength. Table 4 gives the experimental open-hole compression data for a constant width and different d/w values; all specimens failed from the hole along a line almost perpendicular to the loading axis.

3.3. Compression after impact

Each panel was impacted with a known energy level of between 3.5 and 28 J. An energy level of 28 J was too large for the panels of 16-plies as it caused too much damage to

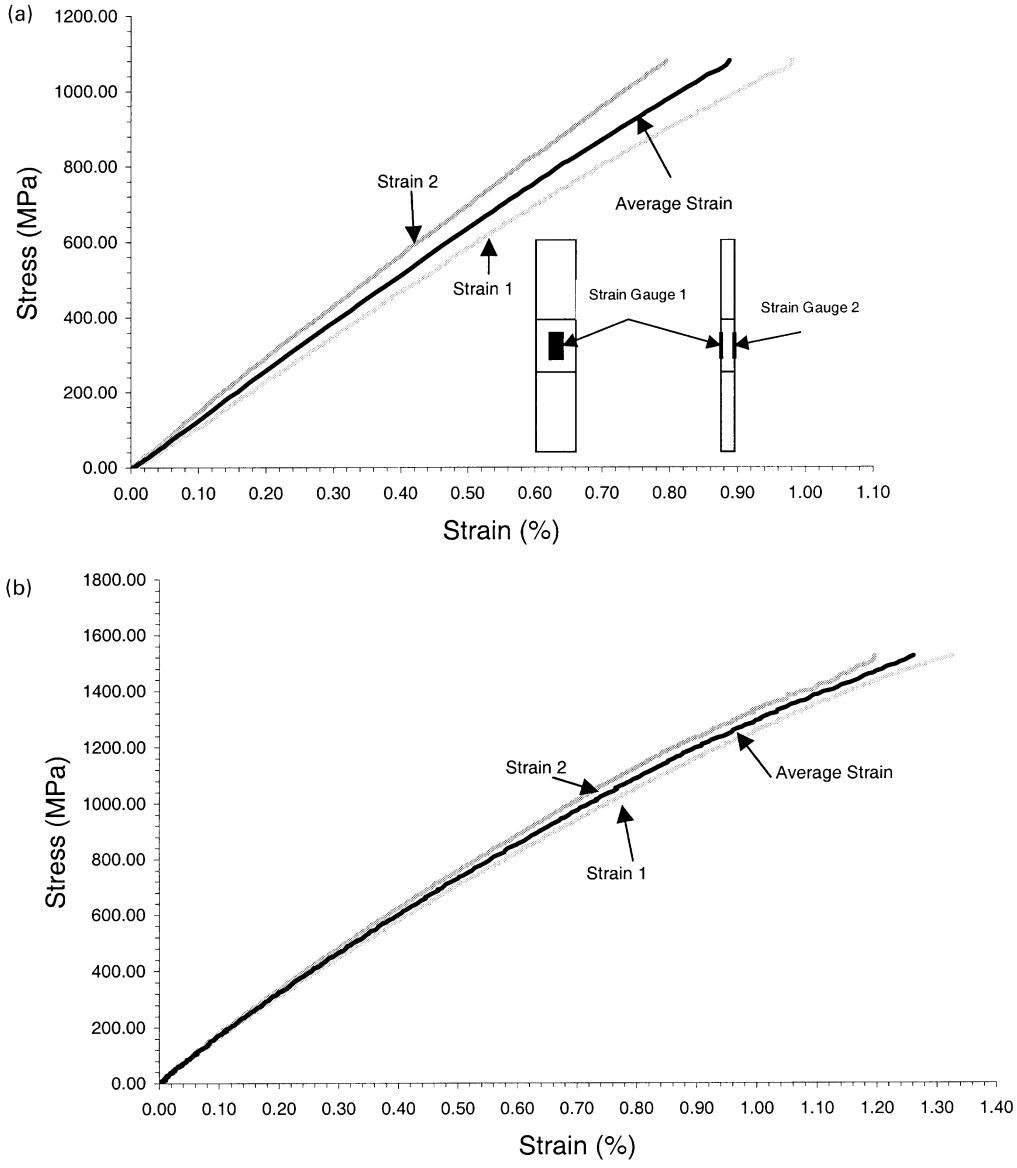

Fig. 2. Typical stress–strain curves for T800/924C unidirectional material performing Celanese-type compression tests: (a) with modified Celanese jig showing a large amount of bending; (b) with original Celanese jig showing a reduced amount of bending.

Table 3
Mean plain compression strengths

Lay-up	σ_{un}^{exp} (MPa)
1	602 [8]
2	636 [5]
3	478 [5]
4	853 [9]
5	881 [10]
6	718 [10]
7	660 [10]
8	392[a] [5]

[a] Value low due to premature bending of test-piece.

make this test useful. In addition, an energy level of 3.5 J was too insignificant to encourage the test-piece to fail at the impact site. It is for these reasons that most data has been obtained from 7 J impacts. The residual compressive strengths of the test-pieces cut from the different panels are recorded in Table 5.

Table 4
Open-hole compression strengths for different d/w ratios ($w = 35$ mm)

Lay-up	d/w	σ_{n}^{exp} MPa
1	0.142	300 [5]
2	0.167	390 [6]
4	0.200	382 [9]
8	0.142	335 [5]

Table 5
Compression after impact results for several multidirectional lay-ups

	σ_{CAI}^{exp} (MPa) 3.5 J	7 J	10 J	28 J
Lay-up 1		260 [8]		
Lay-up 3				192 [6]
Lay-up 4	397 [9]	293 [9], 344 [10]		
Lay-up 5		318 [10]		
Lay-up 6		298 [10]		
Lay-up 7		312 [10]		
Lay-up 8		452	349	

The extent of damage caused by the impact was observed by C-scan and X-ray radiography of the panel. The actual area of damage varied with type of material and lay-up. Typical C-scans and X-radiographs of impact damage are given in Fig. 3a and b. These show the spread of damage around the impact site. Lower energies gave near-circular areas of damage whereas higher energies gave a more elliptical shape. X-radiographs showed more clearly the density of damage that was smaller and more intense than the C-scans, and gave a better approximation to the size of an equivalent hole required in the strength model.

The intensity of the dark region in the radiograph (Fig. 3b), is a measure of the extent of severe damage in the specimen. Sectioning/polishing and de-ply studies by Hitchen and Kemp [10] on lay-ups 4–7 (T800/924 system) revealed that in the very dark area fibre breakage and delaminations exist in almost all interfaces through the thickness of the laminate. The area of damage that is to be modelled as an open-hole must be approximated from this intense region [2]. The lighter region in Fig. 3b corresponds to the splitting and delamination of the back face rather than internal damage.

3.4. Compression failure mechanism

Due to the lower matrix resin stiffness of modern carbon fibre reinforced plastic (CFRP) materials, compression failure occurs as a result of fibre microbuckling rather than by fibre shear failure. This failure mechanism initiates at free edges where the fibres are unsupported, or at a material imperfection such as resin-rich regions, voids or fibre waviness [11]. The 0° fibres microbuckle and break at two points within a narrow band creating a kink band, which is inclined to the horizontal axis at an angle, β. Failure occurs when the microbuckle growth becomes unstable. Typical values for fibre waviness and kink band inclination are between 2 and 3°, and between 5 and 25°, respectively [4,7]. These typical values are used in theoretical strength predictions, presented in the following section. Fig. 1a and b shows a schematic diagram and a micrograph of fibre microbuckling. This fibre instability failure mode occurs in all unidirectional and multidirectional laminates with or without open holes/impact damage.

4. Theoretical predictions

4.1. Model details

The cohesive zone model by Soutis et al. [1] has been implemented into a user friendly composites design tool (Composite Compressive Strength Modeller, CCSM), Sutcliffe et al. [12] with a Windows™ interface. This software uses several stress-based and fracture-based theoretical models to predict deformation and failure behaviour of composite materials. These models estimate the strength of individual lamina under in-plane stresses on a ply-by-ply basis. The software does not consider interlaminar stresses.

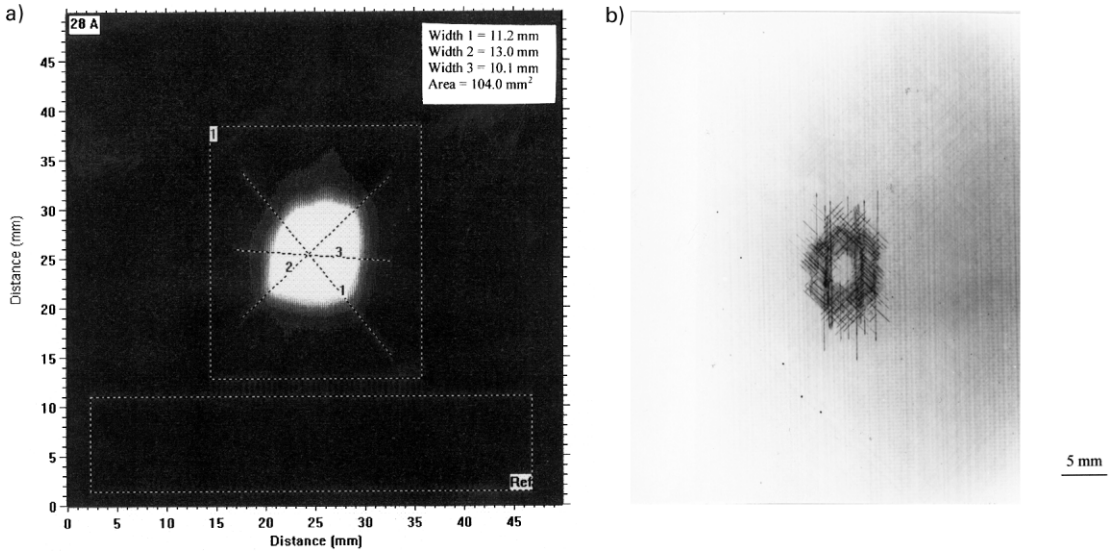

Fig. 3. (a) Typical C-scan and (b) typical X-radiograph for impact damage.

Table 6
Theoretical predictions for each of the five lay-ups based on a width of 50 mm and a K_c value of 45 MPa$\sqrt{m}$. Results have been normalised with the unnotched compressive strength, σ_{un}^{th}

d/w	Lay-up 1 σ_n^{th} (MPa)	$\sigma_n^{th}/\sigma^{th}{}_{un}$	Lay-up 2 σ_n^{th} (MPa)	$\sigma_n^{th}/\sigma_{un}^{th}$	Lay-up 3 σ_n^{th} (MPa)	$\sigma^{th}n/\sigma_{un}^{th}$	Lay-up 4 σ_n^{th} (MPa)	$\sigma^{th}n/\sigma_{un}^{th}$	Lay-up 8 σ_n^{th} (MPa)	$\sigma^{th}n/\sigma_{un}^{th}$
0.00	566	1	759	1	566	1	654	1	578	1
0.10	373	0.66	419	0.55	373	0.66	397	0.61	377	0.65
0.20	305	0.54	346	0.46	305	0.54	324	0.50	307	0.53
0.25	281	0.50	322	0.42	281	0.50	300	0.46	284	0.49
0.30	261	0.46	300	0.40	261	0.46	279	0.43	263	0.46

The Budiansky–Fleck [13] and Soutis–Fleck [1] failure criteria are used in the computer code in combination with classical laminate theory to predict first-ply failure strength of the laminate subjected to in-plane compression. It should be recognised that composite laminates usually contain plies of several orientations, and so the ultimate tensile failure strength is likely to be greater than first-ply failure strength. However, under compressive loading, failure of the 0° plies due to fibre microbuckling usually results in immediate laminate fracture [1].

The parameters required to predict compressive strengths are matrix shear strength, k, fibre waviness, ϕ and kink band inclination angle, β, as well as the elastic properties of the material (Poisson's ratio, ν, longitudinal modulus, E_{11}, transverse modulus, E_{22}, and shear modulus, G_{12}). For open-hole or notched examples, specimen geometry (plate width, w and hole diameter, d) and fracture toughness K_{1c}, are also required. This data may be approximated with typical suggested values, or may be determined experimentally.

Characterisation data for the T800/924 system is contained in the built-in database within the software. Data for IMS/M21 has been approximated or taken from other sources as indicated. In both cases, the value of in-plane fracture toughness, K_{1c}, has been taken equal to 45 MPa$\sqrt{m}$ [14,15]. Strictly speaking it should be determined experimentally, and Ref. [14] describes the method that involves testing centre-cracked specimens in compression. The specimens used were 245 mm long by 50 mm wide with central splits pre-sharpened by a razor blade. More recently, Soutis and Curtis [16] presented a new method for the calculation of the fracture energy associated with fibre microbuckling, which for the systems examined in this study results to K_{1c} values of between 40 and 50 MPa$\sqrt{m}$. Hence an approximate value of 45 MPa$\sqrt{m}$ is not unreasonable.

Values for fibre waviness, ϕ and kink band inclination, β (Fig. 1), have been taken as 3 and 25°, respectively, for both materials. Strength predictions are also influenced by the value of the laminate width, w, as well as the ratio d/w.

4.2. Open-hole compression strength (OHC)

Theoretical predictions, σ_n^{th}, for the open-hole compressive strength for lay-ups 1–4 and 8 have been calculated using the CCSM software [12] and are recorded in Table 6. It can be seen from Table 6 (lay-ups 1 and 3) that the order of plies (stacking sequence) does not affect the theoretical prediction when the same number of plies of each orientation are considered. This is because the model ignores ply interaction (and through thickness) effects that may affect the measured data. Fig. 4 shows graphically the variation in normalised residual strength versus d/w for two different lay-ups. From this graph it can be seen that for the two lay-ups studied, the residual strength is reduced substantially with increasing hole diameter and for $d/w = 0.4$ is only 40% of the unnotched strength.

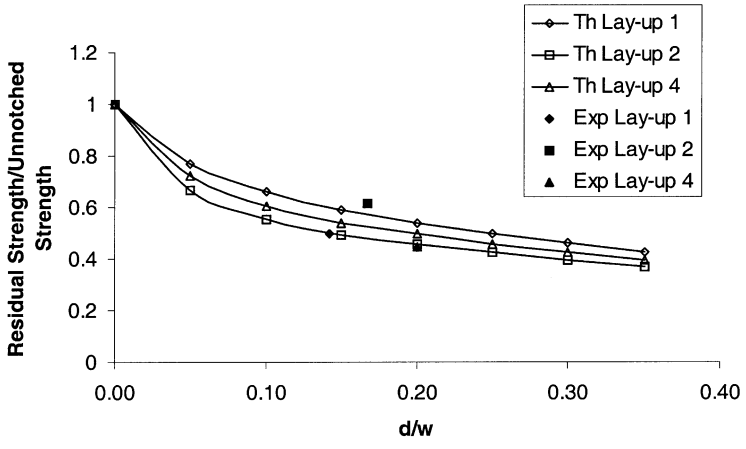

Fig. 4. Graph showing variation in theoretical prediction and experimental values of residual strength versus d/w ratio of lay-ups 1, 2 and 4.

Table 7
Theoretical predictions for OHC for known hole diameter

Lay-up	w (mm)	d (mm)	σ_n^{th} (MPa)	σ_n^{exp} (MPa)	Difference (%)
1	35	5	362	299	17.4
2	36	6	401	390	2.7
4	25	5	407	382	6.1
5	35	5	376	335	10.9

Table 7 gives the theoretical predictions for open-hole compressive strength, σ_n^{th} along with the corresponding experimental values, σ_n^{exp}. The theory over-predicts the strength by between 2.7 and 17.4%, suggesting that the assumed value of 45 MPa$\sqrt{m}$ for K_{1c} is rather high. A more accurate value of K_{1c} could be obtained by using the method described by Soutis and Curtis [16].

4.3. Compression after impact strength (CAI)

In order to predict the residual strength of an impact-damaged coupon, the area of impact damage was modelled as an equivalent hole. The equivalent hole is assumed to be equal to the delamination width, a, measured from X-ray radiographs and/or C-scans. Hitchen and Kemp [10] showed that all T800H/924C panels tested within their programme contained a region of severe damage around the site of impact. The study of X-radiographs of the damage showed that the region of most intensity was limited to a small area (Fig. 3b). This area of maximum intensity is the region that equates to an equivalent hole and contains a large amount of broken fibres. The hole diameter could also be obtained from the ultrasonic C-scan image (Fig. 3a), but this is less easy as it is difficult to distinguish between internal and back-face damage. The apparent hole size would then be the maximum extent of delaminations from all interfaces. When this larger 'hole' was used in the model, the residual strength was underestimated by approximately 10–20% [2].

Table 8 gives theoretical predictions for residual compressive strength after impact. In most cases the value of a has been determined from X-radiographs, but in some cases this was not possible, and instead has been determined from given values of a/w and w. In two cases no X-radiographs were taken and so estimates of a and a/w have been made from experimental strength values. Experimental results are also presented in Table 8 and it can be seen that in all but one case, the theory over-predicts the residual strength by between 2.6 and 21%. One lay-up is under-predicted by 18.5% suggesting that the strength reduction due to impact damage is not as severe as the equivalent open-hole assumed in the CCSM model; a region with reduced stiffness properties (a soft inclusion) could give a better correlation with the measured data.

Table 8
Comparison of theoretical predictions for residual compressive strength after impact (σ_{CAI}^{th}) with experimental values (σ_{CAI}^{exp}). The value of a has been determined from X-radiographs

Lay-up	a (mm)	a/w	σ_{CAI}^{th} (MPa)	σ_{CAI}^{exp} (MPa)	Difference (%)
1	9	0.18	309	260 [8]	15.8
3	50[a]	0.502[b]	162	192 [5]	− 18.5
4	7[c]	0.14	371	293 [9]	21
4	4[c]	0.08	433	397 [9]	8.3
4	6	0.12	388	344 [10]	11.3
5	7	0.14	371	318 [10]	14.3
6	13	0.26	306	298 [10]	2.6
7	10	0.20	334	312 [10]	6.6
8	2.1[a]	0.07[d]		452	
8	6[a]	0.20[d]		349	

[a] Determined from known value of w.
[b] Given value of a/w.
[c] Difficult to determine from X-radiograph.
[d] Predicted by using experimental strength value.

5. Concluding remarks

It can be seen from the results presented in this paper that the theoretical model developed for predicting the open-hole compressive strength of composites can be used to estimate compression after impact strength. X-ray radiographs of the damaged area are required in order to establish an equivalent hole diameter. With knowledge of this diameter and the width of the laminate or test-piece, the residual strength can be predicted by the Sutcliffe et al. computer program [12] based on the Soutis et al. [1] cohesive zone model. Typical values for in-plane fracture toughness and fibre imperfections will need to be used if this information is not already known.

Whilst the model has not yet been thoroughly tested, the potential for it to be used as a tool to characterise the notch sensitivity and damage tolerance of composite laminates is encouraging. Further work is required to estimate the size of impact damage, which will eliminate the need for X-ray radiography.

Acknowledgements

This work was carried out as part of Technology Group 4 of the MOD Corporate Research Programme and the DTI CARAD programme. The authors also wish to acknowledge Mr G. MacKenzie, Mr K. Denham, Mrs A. Dewar, all from DERA, Farnborough for additional help with this work.

References

[1] Soutis C, Fleck NA, Smith PA. Failure prediction technique for compression loaded carbon fibre-epoxy laminate with open holes. J Comput Mater 1991;25(11):1476–98.
[2] Soutis C, Curtis PT. Prediction of the post-impact compressive strength of CFRP laminated composites. Compos Sci Technol 1996;56(6):677–84.
[3] Curtis PT. CRAG Test Methods for the Measurements of the Engineering Properties of Fibre Reinforced Plastics. Royal Aerospace Establishment Technical Report TR88012, 1988.

[4] Fleck NA. Compressive failure of fibre composites. In: Hutchinson JW, Wu TY, editors. Advance in applied mechanics, vol. 34. New York: Academic Press, 1997. p. 43.
[5] Hawyes VJ, Soutis C, Curtis PT. A Study of the Compressive Behaviour of CFRPs in Different Environmental Conditions. DERA Technical Report DERA/MSS/MSMA2/TR990339, 1999.
[6] Soutis C, Smith FC, Matthews FL. Predicting the compressive engineering performance of carbon fibre-reinforced plastics. Composites, Part A 2000;31(6):531–6.
[7] Soutis C. Compressive strength of unidirectional composites: measurement and prediction. In: Hooper SJ, editor. Composite materials: testing and design, ASTM STP 1242, vol. 13. American Society for Testing Materials, 1997. Lancaster, PA: Technomic, p. 168–176.
[8] Curtis PT, Gates J, Molyneux CG. Impact Damage Growth in Carbon Fibre Composites. Defence Research Agency Report 93009, February 1993.
[9] Curtis PT, Browne M, Desport A. Cost Effective High Performance Composites. Defence Research Agency Technical Report TR9 2009, 1992.
[10] Hitchen SA, Kemp RMJ. The Effect of Stacking Sequence and Layer Thickness on the Compressive Behaviour of Carbon Composite Materials. DERA Technical Report DRA/AS/MS/TR94003/1, February 1994.
[11] Soutis C, Turkmen D. Moisture and temperature effects of the compressive failure of CFRP unidirectional laminates. J Comput Mater 1997;31(8):832–49.
[12] Sutcliffe MPF, Xin XJ, Fleck NA, Curtis PT. Composite Compressive Strength Modeller (CCSM), version 1.4, A User's Manual. Cambridge University Engineering Department, CUED MICROMECH/TR35, 1999.
[13] Budiansky B, Fleck NA. Compressive failure of fibre composites. J Mech Phys Solids 1993;41(1):183.
[14] Soutis C, Curtis PT, Fleck NA. Compressive failure of notched carbon fibre composites. Proc R Soc Lond Ser A 1993;440:241–56.
[15] Soutis C, Edge EC. A method for the production of carpet plots for notched compression strength of carbon fibre reinforced plastic multidirectional laminates. Proc Instn Mech Eng; 211(G); J Aero Eng: 251-261.
[16] Soutis C, Curtis PT. A method for predicting the fracture toughness of cfrp laminates failing by fibre microbuckling. Composites, Part A 2000;31(7):733–40.